Chapter 5
At a Point Infiltration Models for Calculating Runoff

CHAPTER 5: AT A POINT INFILTRATION MODELS FOR CALCULATING RUNOFF

Infiltration is the movement of water into the soil under the driving forces of gravity and capillarity, and limited by viscous forces involved in the flow into soil pores as quantified in terms of permeability or hydraulic conductivity. The *infiltration rate*, f, is the rate at which this process occurs. The infiltration rate actually experienced in a given soil depends on the amount and distribution of soil moisture and on the availability of water at the surface. There is a maximum rate at which the soil in a given condition can absorb water. This upper limit is called the *infiltration capacity*, f_c. Note that this is a rate, not a depth quantity. It is a limitation on the rate at which water can move into the ground. If surface water input is less than infiltration capacity, the infiltration rate will be equal to the surface water input rate, w. If rainfall intensity exceeds the ability of the soil to absorb moisture, infiltration occurs at the infiltration capacity rate. Therefore to calculate the actual infiltration rate, f, is the lesser of f_c or w. Water that does not infiltrate collects on the ground surface and contributes to surface detention or runoff (Figure 35). The surface overland flow runoff rate, R, is the excess surface water input that does not infiltrate.

$$R = w - f \tag{28}$$

This is also often referred to as *precipitation excess*.

The infiltration capacity declines rapidly during the early part of a storm and reaches an approximately constant steady state value after a few hours (Figure 7). The focus of this section on at a point infiltration models for calculating runoff is on how to calculate runoff accounting for the reduction of infiltration capacity. We use accumulated infiltration depth, F, as an independent variable and write infiltration capacity as a decreasing function $f_c(F)$, then as F increases with time f_c is reduced. f_c may be a gradually decreasing function, or a threshold function, as in the case of saturation excess runoff where there is a finite soil moisture deficit that can accommodate surface water input.

Several processes combine to reduce the infiltration capacity. The filling of fine pores with water reduces capillary forces drawing water into pores and fills the storage potential of the soil. Clay swells as it becomes wetter and the size of pores is reduced. The impact of

raindrops breaks up soil aggregates, splashing fine particles over the surface and washing them into pores where they impede the entry of water. Coarse-textured soils such as sands have large pores down which water can easily drain, while the exceedingly fine pores in clays retard drainage. If the soil particles are held together in aggregates by organic matter or a small amount of clay, the soil will have a loose, friable structure that will allow rapid infiltration and drainage.
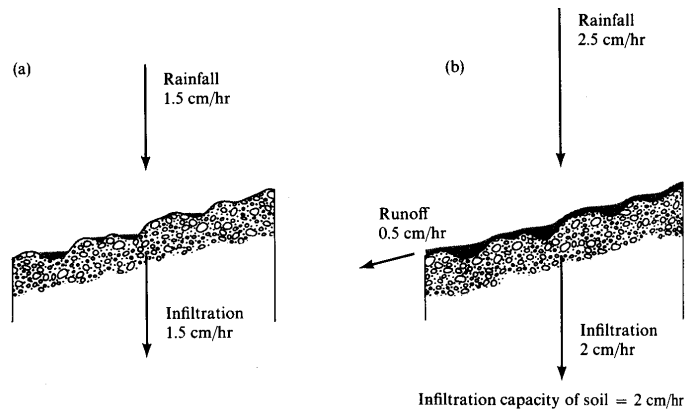
Figure 35. Surface Runoff occurs when surface water input exceeds infiltration capacity. (a) Infiltration rate = rainfall rate which is less than infiltration capacity. (b) Runoff rate = Rainfall intensity – Infiltration capacity (from Water in Environmental Planning, Dunne and Leopold, 1978)

The depth of the soil profile and its initial moisture content are important determinants of how much infiltrating water can be stored in the soil before saturation is reached. Deep, well-drained, coarse-textured soils with large organic matter content will tend to have high infiltration capacities, whereas shallow soil profiles developed in clays will accept only low rates and volumes of infiltration.

Vegetation cover and land use are very important controls of infiltration. Vegetation and litter protect soil from packing by raindrops and provide organic matter for binding soil particles together in open aggregates. Soil fauna that live on the organic matter assist this process by churning together the mineral particles and the organic material. The manipulation of vegetation during land use causes large differences in infiltration capacity. In particular, the stripping of forests and their replacement by crops that do not cover the ground efficiently and do not maintain a high organic content in the soil often lower the infiltration capacity drastically. Soil surfaces trampled by livestock or compacted by vehicles also have reduced

infiltration capacity. The most extreme reduction of infiltration capacity, of course, involves the replacement of vegetation by an asphalt or concrete cover in urban areas. In large rainstorms it is the final, steady state rate of infiltration that largely determines the amount of surface runoff that is generated.

The calculation of infiltration at a point combines the physical conservation of mass (water) principle expressed through the continuity equation with quantification of unsaturated flow through soils, expressed by Darcy's equation. Here we will derive the continuity equation then substitute in Darcy's equation to obtain as a result Richard's equation which describes the vertical movement of water through unsaturated soil. Figure 36 shows a control volume in an unsaturated porous medium. Consider flow only in the vertical direction. The specific discharge across the bottom surface into the volume is denoted as q, and the outflow across the top surface is denoted as q+Δq. The volumetric flux is specific discharge times cross sectional area, $A = \Delta x \cdot \Delta y$. The volume of water in the control volume is the moisture content times the total volume (equation 7), here $V = \Delta x \cdot \Delta y \cdot \Delta z$. Therefore we can write

Change in Storage = (Inflow rate – Outflow rate) x (time interval)

$$\Delta\theta\ \Delta x\ \Delta y\ \Delta z = (q\ \Delta x\ \Delta y - (q+\Delta q)\ \Delta x\ \Delta y)\ \Delta t \tag{29}$$

Dividing by $\Delta x\ \Delta y\ \Delta z\ \Delta t$ and simplifying results in

$$\frac{\Delta\theta}{\Delta t} = -\frac{\Delta q}{\Delta z} \tag{30}$$

Now letting Δz and Δt get smaller and approach 0, as is usual in calculus, we get

$$\frac{\partial\theta}{\partial t} = -\frac{\partial q}{\partial z} \tag{31}$$

This is the continuity equation in one direction (the vertical direction z). In a more general case where flow can be three dimensional, the continuity equation is obtained in a similar fashion as

$$\frac{\partial\theta}{\partial t} = -\left(\frac{\partial q_x}{\partial x} + \frac{\partial q_y}{\partial y} + \frac{\partial q_z}{\partial z}\right) = -\nabla \bullet \underline{q} \tag{32}$$

where the operator ∇ is used as shorthand notation for $\left(\dfrac{\partial}{\partial x}, \dfrac{\partial}{\partial y}, \dfrac{\partial}{\partial z}\right)$ and $\underline{q}$ denotes the specific discharge vector (q_x, q_y, q_z) with component in each coordinate direction.
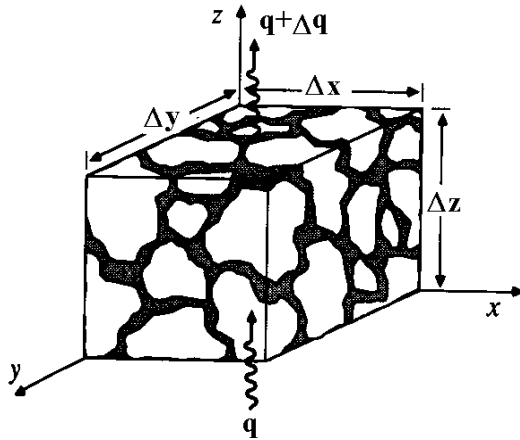
Figure 36. Control volume for development of the continuity equation in an unsaturated porous medium (from Chow et al., 1988).

Substituting Darcy's equation (16) into (31) gives

$$\frac{\partial \theta}{\partial t} = \frac{\partial}{\partial z} K \frac{\partial h}{\partial z} \tag{33}$$

In this equation $h = \psi + z$ (equation 18) resulting in

$$\frac{\partial \theta}{\partial t} = \frac{\partial}{\partial z}\left(K \frac{\partial \psi}{\partial z} + K\right) \tag{34}$$

This equation is known as Richard's equation and it describes the vertical movement of water through unsaturated soil. Although simple appearing, its solution is complicated by the soil moisture characteristic relationships relating moisture content and pressure head $\theta(\psi)$ and Hydraulic conductivity and pressure head or moisture content $K(\psi)$ or $K(\theta)$ discussed above (equations 25, 26, 27 and Figures 29-32). Richard's equation may be written in one of two forms depending on whether we take moisture content, θ, or pressure head, ψ, as the independent variable.

In terms of moisture content, Richard's equation is written

$$\frac{\partial \theta}{\partial t} = \frac{\partial}{\partial z}\left(K(\theta)\frac{\partial \psi(\theta)}{\partial z} + K(\theta) \right)$$

$$= \frac{\partial}{\partial z}\left(K(\theta)\frac{d\psi}{d\theta}\frac{\partial \theta}{\partial z} + K(\theta) \right) \qquad (35)$$

$$= \frac{\partial}{\partial z}\left(D(\theta)\frac{\partial \theta}{\partial z} + K(\theta) \right)$$

In this equation the explicit functional dependence on moisture content, θ, has been shown. The quantity $D(\theta)= K(\theta)\dfrac{d\psi}{d\theta}$ is called the *soil water diffusivity*, because the term involving it is similar to a diffusion term in the diffusion equation. For specific parameterizations of the soil moisture characteristic curves $\psi(\theta)$ and $K(\theta)$, such as equations (25-27), $D(\theta)$ can be derived.

In terms of pressure head, Richard's equation is written

$$\frac{\partial \theta(\psi)}{\partial t} = \frac{d\theta}{d\psi}\frac{\partial \psi}{\partial t} = \frac{\partial}{\partial z}\left(K(\psi)\frac{\partial \psi}{\partial z} + K(\psi) \right)$$

$$C(\psi)\frac{\partial \psi}{\partial t} = \frac{\partial}{\partial z}\left(K(\psi)\frac{\partial \psi}{\partial z} + K(\psi) \right) \qquad (36)$$

As above, in this equation the explicit functional dependence on pressure head, ψ, has been shown. The quantity $C(\psi) = d\theta/d\psi$ is called the *specific moisture capacity*.

Analytic solutions for Richard's equation are known for specific parameterizations of the functions $K(\theta)$ and $D(\theta)$ or $K(\psi)$ and $C(\psi)$ and for specific boundary conditions (see e.g. Philip, 1969; Parlange et al., 1999; Smith et al., 2002). There are also computer codes that implement numerical solutions to Richard's equation. Hydrus 1-D is one such code available from the USDA-ARS Salinity Laboratory (http://www.ussl.ars.usda.gov/models/hydr1d1.HTM) Computational codes based on the moisture content form tend to be better at conserving moisture and dealing with dryer soil conditions. These have problems as saturation is increased because moisture content becomes capped at the porosity and $d\psi/d\theta$ tends to infinity. Computational codes based on the pressure head form are able to

better handle the transition between saturated and unsaturated flow near the water table, but because moisture content is not a specific state variable in their solution, are not as good at conserving mass. Pressure head (and suction) is a continuous function of depth, however in layered soils moisture content is discontinuous at the interface between layers where hydraulic conductivity changes. Computer codes using ψ as the independent variable cope better with these discontinuities. Some approaches to the numerical solution of Richard's equation combine the moisture content and pressure head representations (Celia et al., 1990).

Although Richard's equation is fundamental to the movement of water through unsaturated soil we do not give numerical solutions here, because these are complex and require detailed soils data that are usually not available. Instead we analyze the development of soil moisture versus depth profiles more qualitatively to develop the empirical models used to calculate infiltration.

Consider a block of soil that is homogeneous with water table at depth and initially hydrostatic conditions above the water table (Figure 37). Hydrostatic conditions mean that water is not moving, so in Darcy's equation (16), q=0, dh/dz=0 and therefore the hydraulic head h is constant. Because pressure head ψ is 0 at the water table equation (18) implies that $\psi = -z$ where z is the height above the water table. This gives initial moisture content at each depth z

$$\theta(z) = \theta(\psi = -z) \tag{37}$$

from the soil moisture retention characteristic.

Beginning at time t=0, liquid water begins arriving at the surface at a specified surface water input rate w. This water goes into storage in the layer, increasing its water content. The increase in water content causes an increase in hydraulic conductivity according to the hydraulic conductivity – water content relation for the soil (equations 25, 26, 27). Also because the water content is increased, the absolute value of the negative pressure head is reduced according to the soil moisture characteristic and a downward hydraulic gradient is induced. This results in a flux out of the surface layer in to the next layer down. This process happens successively in each layer as water input continues, resulting in the successive water content profiles at times t_1, t_2 and t_3 shown in Figure 37.
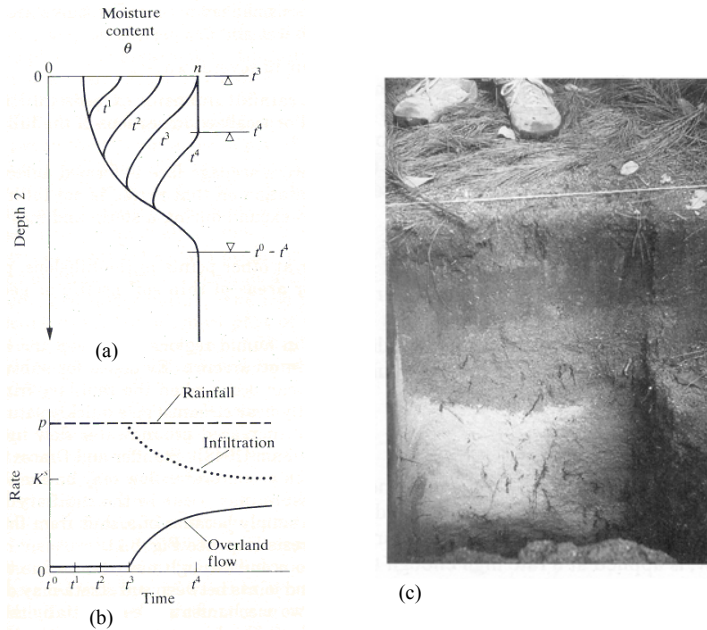
Figure 37. Infiltration excess runoff generation mechanism. (a) Moisture content versus depth profiles and (b) Runoff generation time series. (Bras, Hydrology: An introduction to Hydrologic Science, © 1990. Electronically reproduced by permission of Pearson Education, Inc., Upper Saddle River, New Jersey) (c) Wetting front in a sandy soil exposed after intense rain (Dingman, Physical Hydrology, 2/E, © 2002. Electronically reproduced by permission of Pearson Education, Inc., Upper Saddle River, New Jersey).

Note that the downward hydraulic gradient inducing infiltration is from a combination of the effect of gravity, quantified by the elevation head, and capillary surface tension forces, quantified by the pressure head (negative due to suction) being lower at depth due to lower moisture content. Now if water input rate is greater than the saturated hydraulic conductivity (i.e. $w > K_{sat}$), at some point in time the water content at the surface will reach saturation. At this time the infiltration capacity drops below the surface water input rate and runoff is generated. This is indicated in Figure 37 as time t_3 and is called the *ponding time*. After ponding occurs, water continues to infiltrate and a zone of saturation begins to propagate downward into the soil, as show for t_4 in Figure 37. This wave of soil moisture propagating into the soil (from t_1 to t_4) is referred to as a wetting front. After ponding the infiltration rate is less than the water input

rate and the excess water accumulates at the surface and becomes infiltration excess runoff. As time progresses and the depth of the zone of saturation increases, the contribution of the suction head to the gradient inducing infiltration is reduced, so infiltration capacity is reduced.

The time series of water input, infiltration and surface runoff during this process is depicted in Figure 37b, which shows a reduction in infiltration with time and a corresponding increase in runoff. The necessary conditions for the generation of runoff by the infiltration excess mechanism are (1) a water input rate greater than the saturated hydraulic conductivity of the soil, and (2) a surface water input duration longer than the required ponding time for a given initial soil moisture profile and water input rate.

Now consider a similar situation, but with the water table nearer to the surface as depicted in Figure 38.
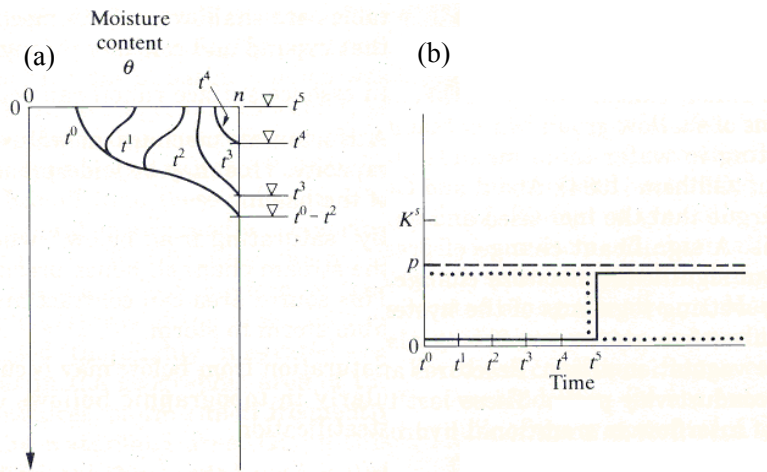
Figure 38. Saturation excess runoff generation mechanism. (a) Moisture content versus depth profiles, and (b) Runoff generation time series. (Bras, Hydrology: An introduction to Hydrologic Science, © 1990. Electronically reproduced by permission of Pearson Education, Inc., Upper Saddle River, New Jersey)

If initial conditions are hydrostatic the initial moisture content is again given by (37). At each depth z, the soil moisture deficit, below saturation is therefore n-θ(z). Integrating this from the water table to the surface we obtain the total soil moisture deficit as

$$D = \int\limits_{0}^{z_w} (n - \theta(z))dz \qquad (38)$$

This defines the total amount of water that can infiltrate into a soil profile. Surface water input to a situation like this again (similar to the infiltration excess case) results in soil moisture profiles at times t_1, t_2, t_3, and t_4, depicted in Figure 38a. However, even if $w < K_{sat}$, a point in time is reached where the accumulated surface water input is equal to D. At this time the soil profile is completely saturated and no further water can infiltrate. Infiltration capacity goes to zero, and all surface water input becomes runoff. This is the saturation excess runoff generation mechanism. The time series of surface water input, infiltration and surface runoff for this mechanism are depicted in Figure 38b.

Note that the infiltration excess and saturation excess mechanisms are not mutually exclusive. One or the other could occur in a given situation given different initial depths to the water table and surface water input rates.

Green–Ampt Model

The Green – Ampt (1911) model is an approximation to the infiltration excess process described above and depicted in Figure 37. In Figure 37 successive soil moisture profiles were shown as curves, with moisture content gradually reducing to the initial conditions below the wetting front. The Green – Ampt model approximates the curved soil moisture profiles, that result in practice, and from solution to Richard's equation, as a sharp interface with saturation conditions, $\theta=n$, above the wetting front and initial moisture content, $\theta=\theta_o$, below the wetting front (Figure 39). The initial moisture content is assumed to be uniform over depth. Let L denote the depth to the wetting front. Denote the difference between initial and saturation moisture contents as $\Delta\theta = n - \theta_o$. Then the depth of infiltrated water following initiation of infiltration is

$$F = L \, \Delta\theta \qquad (39)$$

The datum for the definition of hydraulic head is taken as the surface and an unlimited supply of surface water input is assumed, but with small ponding depth, so the contribution to hydraulic gradient from the depth of ponding at the surface is neglected. Immediately below

the wetting front, at depth just greater than L, the soil is at its initial unsaturated condition, with corresponding suction head $|\psi_f|$. The hydraulic head difference driving infiltration, measured from the surface to just below the wetting front is therefore

$$h = -(L + |\psi_f|) \tag{40}$$

The hydraulic gradient is obtained by dividing this head difference by the distance L between the surface and the wetting front to obtain

$$\frac{dh}{dz} = -\frac{L + |\psi_f|}{L} \tag{41}$$
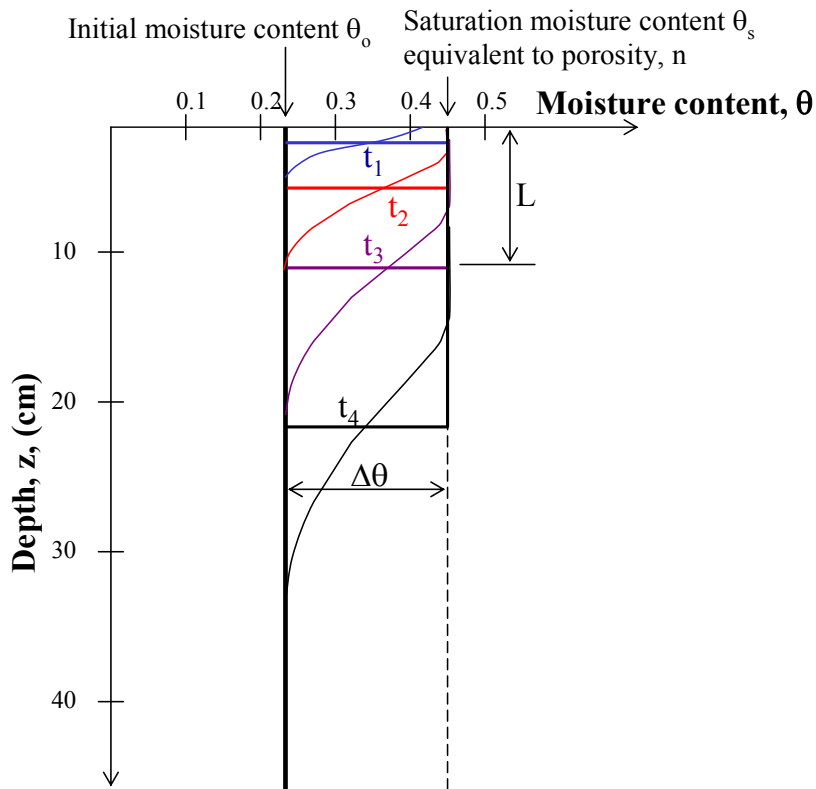
Figure 39. Green–Ampt model idealization of wetting front penetration into a soil profile.

Using this in Darcy's equation (16) gives the infiltration capacity as

$$f_c = K_{sat} \frac{L + |\psi_f|}{L} = K_{sat}\left(1 + \frac{|\psi_f|}{L}\right)$$
$$= K_{sat}\left(1 + \frac{|\psi_f|\Delta\theta}{F}\right) = K_{sat}\left(1 + \frac{P}{F}\right) \tag{42}$$

where in the third expression (39) has been used to express $L = F/\Delta\theta$. This provides an expression for the reduction in infiltration capacity as a function of infiltrated depth $f_c(F)$. The parameters involved are K_{sat} and the product $P = |\psi_f|\Delta\theta$. Using the soil moisture characteristic ψ_f may be estimated as

$$\psi_f = \psi(\theta_o) \tag{43}$$

Values for θ_o may be estimated from field capacity θ_{fc}, or wilting point θ_{pwp}, depending on the antecedent conditions. Rawls et al. (1993) recommended evaluating $|\psi_f|$ from the air entry pressure as

$$|\psi_f| = \frac{2b + 3}{2b + 6}|\psi_a| \tag{44}$$

where $|\psi_a|$ and b are from table 1. The latter simpler approach appears to be justified for most hydrologic purposes (Dingman, 2002). Table 2 gives Green-Ampt infiltration parameters for soil texture classes reported by Rawls et al. (1983).

Given a surface water input rate of w, the cumulative infiltration prior to ponding is $F = wt$. Ponding occurs when infiltration capacity decreases to the point where it equals the water input rate, $f_c = w$. Setting $f_c = w$ in (42) and solving for F one obtains the cumulative infiltration at ponding

Green-Ampt cumulative infiltration at ponding:
$$F_p = \frac{K_{sat}|\psi_f|\Delta\theta}{(w - K_{sat})} \tag{45}$$

The time to ponding is then

Green-Ampt time to ponding:
$$t_p = F_p/w = \frac{K_{sat}|\psi_f|\Delta\theta}{w(w - K_{sat})} \tag{46}$$

Table 2. Green – Ampt infiltration parameters for various soil classes (Rawls et al., 1983). The numbers in parentheses are one standard deviation around the parameter value given.

Soil Texture	Porosity n	Effective porosity θ_e	Wetting front soil suction head $|\psi_f|$ (cm)	Hydraulic conductivity K_{sat} (cm/hr)
Sand	0.437 (0.374-0.500)	0.417 (0.354-0.480)	4.95 (0.97-25.36)	11.78
Loamy sand	0.437 (0.363-0.506)	0.401 (0.329-0.473)	6.13 (1.35-27.94)	2.99
Sandy loam	0.453 (0.351-0.555)	0.412 (0.283-0.541)	11.01 (2.67-45.47)	1.09
Loam	0.463 (0.375-0.551)	0.434 (0.334-0.534)	8.89 (1.33-59.38)	0.34
Silt loam	0.501 (0.420-0.582)	0.486 (0.394-0.578)	16.68 (2.92-95.39)	0.65
Sandy clay loam	0.398 (0.332-0.464)	0.330 (0.235-0.425)	21.85 (4.42-108.0)	0.15
Clay loam	0.464 (0.409-0.519)	0.309 (0.279-0.501)	20.88 (4.79-91.10)	0.1
Silty clay loam	0.471 (0.418-0.524)	0.432 (0.347-0.517)	27.30 (5.67-131.50)	0.1
Sandy clay	0.430 (0.370-0.490)	0.321 (0.207-0.435)	23.90 (4.08-140.2)	0.06
Silty clay	0.479 (0.425-0.533)	0.423 (0.334-0.512)	29.22 (6.13-139.4)	0.05
Clay	0.475 (0.427-0.523)	0.385 (0.269-0.501)	31.63 (6.39-156.5)	0.03

Excel spreadsheet with table in electronic form

To solve for the infiltration that occurs after ponding with the Green Ampt model, recognize that infiltration rate is the derivative of cumulative infiltration, and is limited by the infiltration capacity

$$f(t) = \frac{dF}{dt} = f_c(t) \tag{47}$$

Here the functional dependence on time is explicitly shown. Now using (42) the following differential equation is obtained

$$\frac{dF}{dt} = K_{sat}(1 + \frac{P}{F}) \qquad (48)$$

Using separation of variables this can be integrated from any initial cumulative infiltration depth F_s at time t_s to a final cumulative infiltration depth F at time t

Green-Ampt infiltration under ponded conditions:
$$t - t_s = \frac{F - F_s}{K_{sat}} + \frac{P}{K_{sat}} \ln\left(\frac{F_s + P}{F + P}\right) \qquad (49)$$

There is no explicit expression for F from this equation. However by setting $t_s = t_p$, and $F_s = F_p$ this equation can be solved numerically for F given any arbitrary t (greater than t_p) to give the cumulative infiltration as a function of time.

An important concept that emerges from the Green – Ampt model is that infiltration capacity during a storm decreases as a function of cumulative infiltrated depth. This provides for a decrease in infiltration capacity and increase in runoff ratio with time, consistent with empirical observations. The dependence on cumulative infiltrated depth means that cumulative infiltrated depth may be treated as a state variable and that variable rainfall rates, and hence variable infiltration rates, and consequent variability in the rate at which infiltration capacity is reduced, is modeled quite naturally using the Green – Ampt model. This is referred to as the infiltrability-depth approximation (IDA) (Smith et al., 2002).

In the Horton and Philip infiltration models discussed below the decrease in infiltration capacity is modeled explicitly as a function of time rather than cumulative infiltrated depth. Alternative equivalent solution procedures can be developed using the time compression approach (Mein and Larson, 1973) or the infiltrability-depth approximation. Here the infiltrability-depth approximation is used, because this provides a more natural and physically sound basis for understanding and using this approach.

Horton Model

The Horton infiltration capacity formulation (Horton, 1939; although apparently first proposed by others Gardner and Widstoe, 1921) has an initial infiltration capacity value f_0, for dry or pre-storm conditions. Once surface water input and infiltration commences,

this decreases in an exponential fashion to a steady state infiltration capacity, f_1.

$$f_c(t) = f_1 + (f_0 - f_1)e^{-kt} \qquad (50)$$

Here k is a rate parameter quantifying the rate at which infiltration capacity decreases with time. Eagleson (1970) showed that Horton's equation can be derived from Richard's equation by assuming that K and D are constants independent of the moisture content of the soil. Under these conditions equation (35) reduces to

$$\frac{\partial \theta}{\partial t} = D \frac{\partial^2 \theta}{\partial z^2} \qquad (51)$$

which is the standard form of a diffusion equation and may be solved to yield the moisture content as a function of time and depth. Horton's equation results from solving for the rate of moisture diffusion at the soil surface under specific initial and boundary conditions.

Figure 40 shows the Horton infiltration equation as applied to a given rainfall event. It may be argued that at point t_1 where surface water input rate first exceeds infiltration capacity; the actual infiltration capacity will be larger than that given by $f_c(t_1)$ in the Figure. This is because $f_c(t_1)$ assumes that the infiltration rate has decayed from f_0 due to increased soil moisture from the water that has infiltrated. The cumulative depth of infiltration that has contributed to soil moisture is given by the area under the $f_c(t)$ curve between time 0 and t_1. This is less than the maximum that would have infiltrated were the surface saturated with an unlimited supply of moisture. To account for this discrepancy, the time compression approach (Mein and Larson, 1973) illustrated in Figure 40, was developed. This can be viewed as a shifting of the $f_c(t)$ curve to the right, but is more fundamentally a recasting of equation (50) in terms of cumulative infiltrated depth, F, rather than t, using the infiltrability-depth approximation. Under conditions of unlimited surface water input, the cumulative infiltration up to time t is expressed as

$$F = \int_0^t f_c(t)dt = f_1 t + \frac{(f_0 - f_1)}{k}(1 - e^{-kt}) \qquad (52)$$

Now eliminating t between equation (50) and (52) (by solving (50) for t and substituting in (52)) results in

$$F = \frac{f_0 - f_c}{k} - \frac{f_1}{k}\ln\left(\frac{f_c - f_1}{f_0 - f_1}\right) \tag{53}$$

This is an implicit equation that, given F, can be solved for f_c, i.e. it is an implicit function $f_c(F)$.
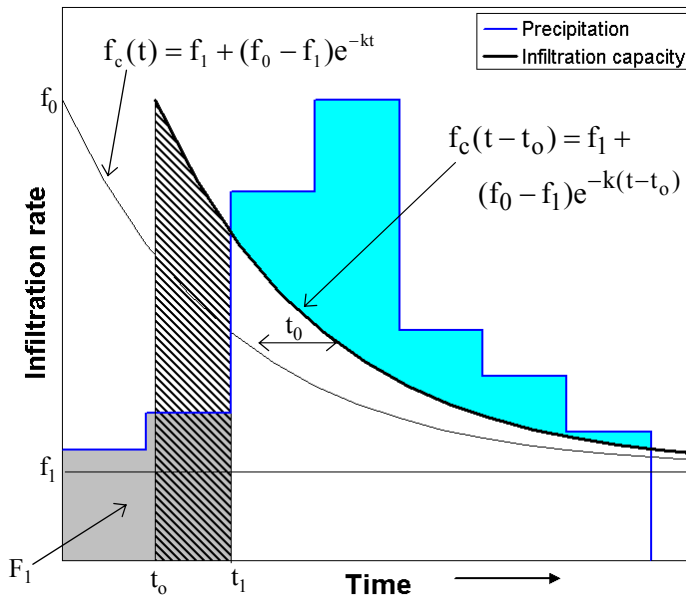
Figure 40. Partition of surface water input into infiltration and runoff using the Horton infiltration equation. Ponding starts at t1. The cumulative depth of water that has infiltrated up to this time is the area F1 (shaded gray). This is less than the maximum possible infiltration up to t1 under the fc(t) curve. To accommodate this the fc(t) curve is shifted in time by an amount to so that the cumulative infiltration from to to t1 (hatched area) equals F1. Runoff is precipitation in excess of fc(t−to) (blue area).

Given a surface water input rate of w, the cumulative infiltration prior to ponding is $F = wt$. Ponding occurs when infiltration capacity decreases to the point where it equals the water input rate, $f_c=w$. Setting $f_c=w$ in (53) one obtains the cumulative infiltration at ponding

Horton cumulative infiltration at ponding:

$$F_p = \frac{f_0 - w}{k} - \frac{f_1}{k} \ln\left(\frac{w - f_1}{f_0 - f_1}\right) \tag{54}$$

The time to ponding is then

Horton time to ponding:

$$t_p = F_p/w = \frac{f_0 - w}{kw} - \frac{f_1}{kw} \ln\left(\frac{w - f_1}{f_0 - f_1}\right) \tag{55}$$

To solve for the infiltration that occurs after ponding with the Horton model, recognize that infiltration rate under ponded conditions is given by f_c, but with the time origin shifted so that the cumulative infiltration F (equation 52) matches the initial cumulative infiltration F_s at an initial time t_s. From (52) t_o is solved implicitly in

$$F_s = f_1(t_s - t_0) + \frac{(f_0 - f_1)}{k}(1 - e^{-k(t_s - t_0)}) \tag{56}$$

Then cumulative infiltration F at any time t ($t > t_s$) can be obtained from

Horton infiltration under ponded conditions:

$$F = f_1(t - t_0) + \frac{(f_0 - f_1)}{k}(1 - e^{-k(t - t_0)}) \tag{57}$$

Philip Model

Philip (1957; 1969) solved Richard's equation under less restrictive conditions (than used by Eagleson (1970) to obtain Horton's equation) by assuming that K and D can vary with the moisture content θ. Philip employed the Boltzmann transformation $B(\theta) = zt^{-1/2}$ to convert (35) into an ordinary differential equation in B, and solved this equation to yield an infinite series for cumulative infiltration F(t). Approximating the solution by retaining only the first two terms in the infinite series results in

$$F(t) = S_p\, t^{1/2} + K_p\, t \tag{58}$$

where S_p is a parameter called *sorptivity*, which is a function of the soil suction potential and K_p is a hydraulic conductivity. Differentiating with respect to time t, we get

$$f_c(t) = \frac{1}{2} S_p t^{-1/2} + K_p \qquad (59)$$

As time increases the first term will decrease to 0 in the limit and $f_c(t)$ will converge to K_p. $\to \infty$, $f_c(t)$ tends to K_p. The two terms in Philip's equation represent the effects of soil suction head and gravity head respectively. As with Horton's equation, this equation can also be recast, using the infiltrability-depth approximation, in terms of cumulative infiltrated depth, F, rather than t, by eliminating t between equations (58) and (59).

$$f_c(F) = K_p + \frac{K_p S_p}{\sqrt{S_p^2 + 4K_p F} - S_p} \qquad (60)$$

In Philip's equation S_p is theoretically related to the wetting front suction (and hence to the initial water content of the soil) and to K_{sat}, and K_p is related to K_{sat}. Rawls et al. (1993; citing Youngs, 1964) suggested that S_p is given by

$$S_p = (2K_{sat} \Delta\theta \,|\, \psi_f \,|)^{1/2} \qquad (61)$$

with $|\psi_f|$ from (43) or (44) and $\Delta\theta = n - \theta_o$, the difference between porosity and initial moisture content. Rawls et al. (1993; citing Youngs, 1964) reports K_p ranging from $K_{sat}/3$ to K_{sat} with K_{sat} the preferred value. $K_p = K_{sat}$ is consistent with the reasoning of the Green – Ampt approach and true for an asymptotic infiltration capacity. However Dingman (2002; citing Sharma et al., 1980) reports that for short time periods smaller values of K_p, generally in the range between 1/3 and 2/3 of K_{sat} better fit measured values.

As for the Horton model, given a surface water input rate of w, the cumulative infiltration prior to ponding is F = wt. Ponding occurs when infiltration capacity decreases to the point where it equals the water input rate, i.e. $f_c = w$. Setting $f_c = w$ in (60) one obtains the cumulative infiltration at ponding

Philip cumulative infiltration at ponding:

$$F_p = \frac{S_p^2(w - K_p/2)}{2(w - K_p)^2} \tag{62}$$

The time to ponding is then

Philip time to ponding:

$$t_p = F_p/w = \frac{S_p^2(w - K_p/2)}{2w(w - K_p)^2} \tag{63}$$

Again, as for the Horton model, to solve for the infiltration that occurs after ponding, recognize that infiltration rate under ponded conditions is given by f_c, but with the time origin shifted so that the cumulative infiltration F (equation 58) matches the initial cumulative infiltration F_s at an initial time t_s. From (58) t_o is solved to be

$$t_0 = t_s - \frac{1}{4K_p^2}\left(\sqrt{S_p^2 + 4K_pF_s} - S_p\right)^2 \tag{64}$$

Then cumulative infiltration F at any time t (t>t_s) can be obtained from

Philip infiltration under ponded conditions:

$$F = S_p(t - t_0)^{1/2} + K_p(t - t_0) \tag{65}$$

Working with at a point infiltration models

In many practical applications the parameters in the Green – Ampt model (K_{sat} and P), Horton model (f_0, f_1 and k) and Philip model (S_p and K_p) are treated simply as empirical parameters whose values are those that best fit infiltration data, or as fitting parameters in relating measured rainfall to measured runoff. The equations (42), (53) and (60) provide different, somewhat physical, somewhat empirical representations of the tendency for infiltration capacity to be reduced in response to the cumulative infiltrated depth.

The functions $f_c(F)$ derived above provide the basis for the calculation of runoff at a point, given a time series of surface water inputs, and the soil conditions, quantified in terms of infiltration model parameters. The problem considered is: Given a surface water input hyetograph, and the parameters of an infiltration

equation, determine the ponding time, the infiltration after ponding occurs, and the runoff generated. The process is illustrated in Figure 41. A discrete representation is used for the surface water input using the time average surface water input in each time interval as input to the calculations. This is the typical way that a precipitation hyetograph is represented. There is flexibility to have the time interval as small as required to represent more detail in the input and output. The output is the runoff generated from excess surface water input over the infiltration capacity integrated over each time interval. Infiltration capacity decreases with time due to its dependence on the cumulative infiltrated depth F, which serves as a state variable through the calculations.
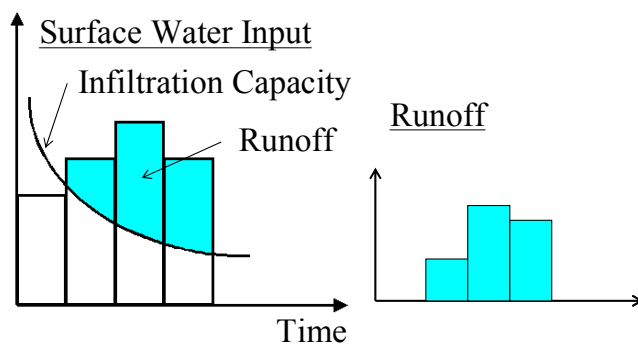
Figure 41. Pulse runoff hyetograph obtained from surface water input hyetograph and variable infiltration capacity.

Figure 42 presents a flow chart for determining infiltration and runoff generated under variable surface water input intensity. Consider a series of time intervals of length Δt. Interval 1 is designated as the interval from t=0 to t=Δt, interval 2 from t=Δt to t=$2\Delta t$ and so on. In general interval i is from t=(i-1)Δt to t=iΔt. The surface water input intensity during the interval is denoted w_t and is taken as constant throughout the interval. The cumulative infiltration depth at the beginning of the interval, representing the initial state, is designated as F_t. The infiltration capacity at the beginning of the interval is then obtained from one of equations (42, 53, 60), corresponding to the Green-Ampt, Horton or Philip models as $f_c(F_t)$. The goal is to, given the infiltrated depth, F_t, at the beginning of a time interval and water input, w_t, during the interval, calculate infiltration f_t during the interval and hence $F_{t+\Delta t}$ at the end of the interval, together with any runoff r_t generated during the time interval. The calculation is initialized with F_0 at the beginning of a storm and proceeds from step to step for the full duration of the

surface water input hyetograph. There are three cases to be considered: (1) ponding occurs throughout the interval; (2) there is no ponding throughout the interval; and (3) ponding begins part-way through the interval. The infiltration capacity is always decreasing or constant with time, so once ponding is established under a given surface water input intensity, it will continue. Ponding cannot cease in the middle of an interval. However ponding may cease at the end of an interval when the surface water input intensity changes. The equations used, based on those derived above, are summarized table 3.

The three infiltration models presented are three of the most popular from a number of at a point infiltration models used in hydrology. Fundamentally there are no advantages of one over the other. The Green-Ampt model provides a precise solution to a relatively crude approximation of infiltration in terms of a sharp wetting front. The Horton model can be justified as a solution to Richard's equation under specific (and practically limiting) assumptions. The Philip model has less limiting assumptions (than Horton) but is a series approximation solution to Richard's equation. Infiltration is a complex process subject to the vagaries of heterogeneity in the soil and preferential flow (as illustrated in Figure 5). Practically, infiltration capacity has the general tendency to decrease with the cumulative depth of infiltrated water and these models provide convenient empirical, but to some extent justifiable in terms of the physical processes involved, equations to parameterize this tendency. The choice of which model to use in any particular setting often amounts to a matter of personal preference and experience and may be based on which one fits the data best, or for which one parameters can be obtained. The Green-Ampt model is popular because Green-Ampt parameters based upon readily available soil texture information has been published (table 2 Rawls et al., 1983). Certain infiltration capacity instruments (Guelph permeameter) have been designed to report their results in terms of parameters for the Philip model.

Three examples, one for each of the models are given to illustrate the procedures involved in calculating runoff using these models. These examples all use the same rainfall input and are designed to produce roughly the same output so that differences between the models can be compared. The examples follow the procedure given in the flow chart (Figure 42) and use the equations summarized in table 3 that were derived above.

Initialize: at t $= 0$, $F_t = 0$

A Calculate infiltration capacity f_c from F_t, column 1 of table.

Is $f_c \leq w_t$

$f_c \leq w_t$

$f_c > w_t$

B Ponding occurs throughout interval: $F_{t+\Delta t}$ calculated using infiltration under ponded conditions equations with $t_s = t$ and $F_s = F_t$. Column 3.

C No ponding at the beginning of the interval. Calculate tentative values
$$F'_{t+\Delta t} = F_t + w_t \Delta t$$
f'_c from $F'_{t+\Delta t}$ and column 1.

Is $f'_c \leq w_t$

$f'_c \leq w_t$

$f'_c > w_t$

D Ponding starts during the interval. Solve for F_p from w_t, column 2.
$$\Delta t' = (F_p - F_t)/w_t$$
$F_{t+\Delta t}$ calculated using infiltration under ponded conditions equations with $t_s = t + \Delta t'$ and $F_s = F_p$. Column 3.

E No ponding throughout interval
$$F_{t+\Delta t} = F'_{t+\Delta t}$$

F Infiltration is $f_t = F_{t+\Delta t} - F_t$
Runoff generated is $r_t = w_t \Delta t - f_t$

G Increment time t$= t + \Delta t$

Figure 42. Flow chart for determining infiltration and runoff generated under variable surface water input intensity.

Table 3. Equations for variable surface water input intensity infiltration calculation.

	Infiltration capacity	Cumulative infiltration at ponding	Cumulative infiltration under ponded conditions
Green-Ampt Parameters K_{sat} and P	$f_c = K_{sat}\left(1 + \dfrac{P}{F}\right)$	$F_p = \dfrac{K_{sat}P}{(w - K_{sat})}$ $w > K_{sat}$	$t - t_s = \dfrac{F - F_s}{K_{sat}} + \dfrac{P}{K_{sat}}\ln\left(\dfrac{F_s + P}{F + P}\right)$ Solve implicitly for F
Horton Parameters k, f_o, f_1.	$F = \dfrac{f_o - f_c}{k} - \dfrac{f_1}{k}\ln\left(\dfrac{f_c - f_1}{f_o - f_1}\right)$ Solve implicitly for f_c given F	$F_p = \dfrac{f_o - w}{k} - \dfrac{f_1}{k}\ln\left(\dfrac{w - f_1}{f_o - f_1}\right)$ $f_c < w < f_o$	Solve first for time offset t_o in $F_s = f_1(t_s - t_o) + \dfrac{(f_o - f_1)}{k}(1 - e^{-k(t_s - t_o)})$ then $F = f_1(t - t_o) + \dfrac{(f_o - f_1)}{k}(1 - e^{-k(t - t_o)})$
Philip Parameters K_p and S_p	$f_c(F) = K_p + \dfrac{K_p S_p}{\sqrt{S_p^2 + 4K_p F} - S_p}$	$F_p = \dfrac{S_p^2(w - K_p/2)}{2(w - K_p)^2}$ $w > K_p$	Solve first for time offset t_o in $t_o = t_s - \dfrac{1}{4K_p^2}\left(\sqrt{S_p^2 + 4K_p F_s} - S_p\right)^2$ then $F = S_p(t - t_o)^{1/2} + K_p(t - t_o)$

Example 1. Green−Ampt. A rainfall hyetograph is given in column 2 of table 4. If this rain falls on a sandy loam of with initial moisture content equal to the field capacity, determine the runoff hyetograph using the Green − Ampt approach.

Solution. The solution is shown in table 4. From table 2, for a sandy loam, K_{sat} = 1.09 cm/h, n=0.453, θ_e = 0.412 and $|\psi_f|$=11.01 cm. From table 1, $|\psi_a|$=21.8 cm and b=4.9. Table 1 gives different values for K_{sat} and n. It is unclear which values are best to use and the K_{sat} values differ by an order of magnitude. This sort of uncertainty is not uncommon. For the purposes of this example we use the K_{sat} and n values from table 2 because these have been developed specifically for the Green-Ampt model.

The effective porosity, θ_e, reported in table 2 suggests a residual moisture content (see equation 24) θ_r=n-θ_e=0.453-0.412=0.041. The concepts of residual moisture content and field capacity are similar (as noted earlier). The residual moisture content could be used with equations (25) or (26) to obtain moisture content corresponding to a negative pressure head that defines field capacity. However this would be inconsistent because the parameters in table 1 are from fits of the simplified Brooks and Corey functions, that do not contain θ_r as a parameter, as expressed in equation (27), to data.

We invert equation (27) to

$$\theta = n\left(\frac{|\psi|}{|\psi_a|}\right)^{-1/b}$$

and use as a definition of field capacity the moisture content corresponding to pressure head ψ = -340 cm in this equation to obtain θ_{fc} = 0.259. This value is larger than θ_r consistent with field capacity being a moisture content reached after about 3 days of drainage as opposed to residual moisture content being a moisture content below which flow in the soil is not possible.

$|\psi_f|$ could also have been estimated from equation (44) which would give a different value to what we obtained from table 2. This is another not uncommon uncertainty in estimation of parameters. Here for the purposes of this example we use the value from table 2.

We now have the information necessary to calculate the P parameter, $P = |\psi_f|(n-\theta_{fc}) = 2.14$ cm.

The time interval is 15 minutes, $\Delta t = 0.25$ h. Column 2 shows the incremental rainfall in each time interval. The rainfall intensity in column 3 is found from column 2 by dividing by Δt (0.25 h).

With this information we now work through the flowchart (Figure 42). Initially $F = 0$, so $f_c = \infty$ (from 42) and ponding does not occur at time 0. Hence we move from box A to box C in the flowchart:

$$F'_{t+\Delta t} = F_t + w_t \Delta t = 0 + 0.3 = 0.3 \, \text{cm}$$

This is the preliminary cumulative infiltration under the assumption of no ponding. The corresponding value of $f'_{t+\Delta t}$ is (from 42)

$$f'_{t+\Delta t} = K_{sat}\left(1 + \frac{P}{F}\right) = 1.09\left(1 + \frac{2.14}{0.3}\right) = 8.867 \, \text{cm}/\text{h}$$

as shown in column 7 of the table. This value is greater than w_t; therefore no ponding occurs during this interval and moving on to box E the cumulative infiltration is set to the preliminary value $F_{t+\Delta t} = F'_{t+\Delta t}$ as shown in column 11. Box F gives the infiltration (column 13) and runoff (column 14). The calculation then proceeds to box G where time is incremented and back to box A for the next time step. The same sequence is followed for the first three time steps where it is found that ponding does not occur up to 0.75 hours of rainfall.

During the fourth time interval (starting at 0.75 hours)

$$f'_{t+\Delta t} = K_{sat}\left(1 + \frac{P}{F}\right) = 1.09\left(1 + \frac{2.14}{1.8}\right) = 2.386 \, \text{cm}/\text{h}$$

as shown in column 7 of the table. This value is less that $w_t = 2.4$ cm/h for the interval from 0.75 to 1 h so ponding starts during this interval. Following the preliminary infiltration rate calculation in box C the calculation proceeds to box D. The cumulative infiltration at ponding is given by (45, also table 3 column2)

$$F_p = \frac{K_{sat}P}{(w - K_{sat})} = \frac{1.09 \times 2.14}{2.4 - 1.09} = 1.781 \text{ cm}$$

The partial time interval required for ponding is

$$\Delta t' = (F_p\text{-}F_t)/w_t = (1.781 - 1.2)/2.4 = 0.242 \text{ h.}$$

Ponding therefore starts at $0.75 + 0.242 = 0.992$ h as shown in column 9. Infiltration under ponded conditions occurs from 0.992 h to 1.0 h. The cumulative infiltration at the end of this interval is obtained by solving equation (49, column3 table 3) for F. Define the function

$$g(F) = t - t_s - \frac{F - F_s}{K_{sat}} - \frac{P}{K_{sat}} \ln\left(\frac{F_s + P}{F + P} \right)$$

and solve numerically for $g(F) = 0$. This is accomplished easily using the Solver function in Excel, or using a numerical solution method such as Newton Rhapson (Gerald, 1978). $g(F)$ is shown in column 12. This results in

$$F_{t+\Delta t} = 1.79995 \text{ cm.}$$

(This numerical precision is not warranted but is retained here for clarity to indicate that this number is less than 1.8.) The infiltration in this time interval is therefore (column 13)

$$f_t = F_{t+\Delta t} - F_t = 1.79995 - 1.2 = 0.59995 \text{ cm}$$

The rainfall is 0.6 cm so the runoff generated is 0.6-0.59995 = 0.00005 cm (column 14). Practically this runoff is 0.

At the start of the fifth time interval (time = 1 h) the cumulative infiltration is 1.79995 cm. This leads to an infiltration capacity

$$f_c = K_{sat}\left(1 + \frac{P}{F}\right) = 1.09\left(1 + \frac{2.14}{1.79995}\right) = 2.386 \text{ cm/h}$$

This is already less than the rainfall rate (2.8 cm/h) for the fifth time interval so the calculation proceeds through box B on the flowchart. The procedure is exactly the same as for box D, except that the starting values F_s and t_s are taken as the beginning of the time step

values (columns 8 and 10). There is no need to solve for the time when ponding starts during the interval. Numerical solution of g(F) = 0 is used to obtain $F_{t+\Delta t}$ given in column 11.

Similarly, at the start of the sixth time interval (time=1.25 h) the cumulative infiltration is 2.354 cm which with equation (42) leads to f_c = 2.081 cm/h (column 5), already less than the rainfall rate (3.2 cm/h) so the calculation proceeds through box B on the flowchart to obtain the cumulative infiltration reported in column 11 and infiltration and runoff reported in columns 13 and 14.

During the seventh time interval (starting at time =1.5 h) the rainfall rate reduces to 1.6 cm/h. At the start of this interval the cumulative infiltration is 2.851 cm and using equation (42) the infiltration capacity is 1.908 cm/h (column 5). This is more than the rainfall rate, so in this time interval ponding ceases and all rainfall infiltrates (at least initially). The calculation enters box C of the flowchart and the preliminary cumulative infiltration at the end of the time interval is calculated (column 6)

$$F'_{t+\Delta t} = F_t + w_t \Delta t = 2.851 + 0.4 = 3.251 \text{cm}$$

Using this value in equation (42) gives (column 7) f_c'=1.808 cm/h. This is more than the rainfall rate so no ponding in this interval is confirmed, and the calculation proceeds through box E, F, G, resulting in no runoff being generated.

During the eighth time interval (starting at time =1.75 h) the rainfall rate increases to 2.4 cm/h. At the start of this interval the cumulative infiltration is 3.251 cm and using equation (42) (or recognizing the result from above) the infiltration capacity (column 5) is f_c=1.808 cm/h. This is less than the rainfall rate, so ponding occurs again in this time interval, starting at the beginning of the time interval, and the calculation proceeds through box B similar to the fifth and sixth time intervals above, with infiltration and runoff given in columns 13 and 14.

The last time interval (starting at time = 2.00 h) is similar with ponding throughout the interval. Figure 43 illustrates the rainfall hyetograph, infiltration capacity and runoff generated from this example.
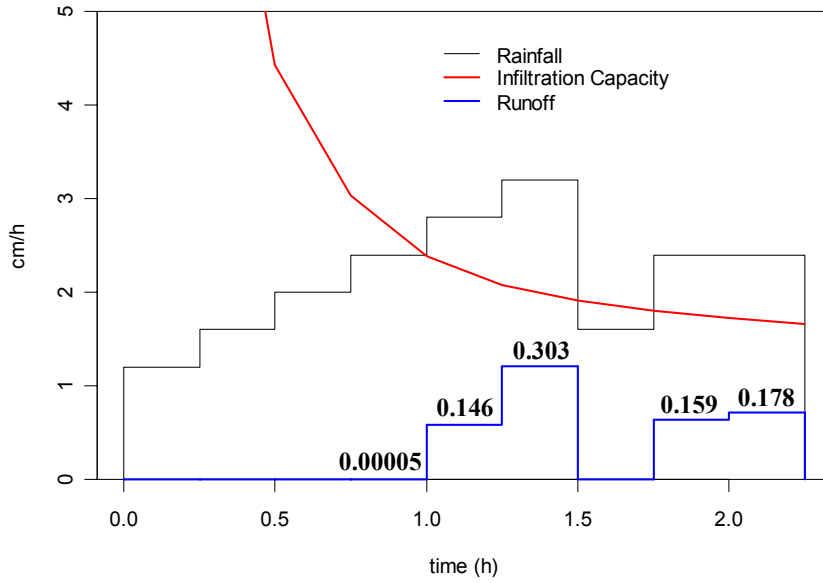
Figure 43. Rainfall Hyetograph, Infiltration Capacity and Runoff Generated in Example 1. Numbers are infiltration in cm in each interval.

Table 4. Calculation of runoff using the Green–Ampt infiltration equation.

Column	1	2	3	4	5	6	7	8	9	10	11	12	13	14
	Time	Incremental Rainfall	Rainfall Intensity	F_t	f_c	F'	f_c'	F_p or F_s	dt'	t_s	$F_{t+\Delta t}$	g(F)	Infiltration	Runoff
	(h)	(cm)	(cm/h)	(cm)	(cm/h)	(cm)	(cm/h)	(cm)	(h)	(h)	(cm)		(cm)	(cm)
	0	0.3	1.2	0	∞	0.300	8.867				0.300		**0.300**	**0.000**
	0.25	0.4	1.6	0.300	8.867	0.700	4.423				0.700		**0.400**	**0.000**
	0.50	0.5	2	0.700	4.423	1.200	3.034				1.200		**0.500**	**0.000**
Ponding 0.75	0.75	0.6	2.4	1.200	3.034	1.800	2.386	1.781	0.242	0.992	1.79995	0.000	**0.59995**	**0.00005**
1.00	1.00	0.7	2.8	1.800	2.386			1.800	0.000	1.000	2.354	0.000	**0.554**	**0.146**
1.25	1.25	0.8	3.2	2.354	2.081			2.354	0.000	1.250	2.851	0.000	**0.497**	**0.303**
Ponding 1.50	1.50	0.4	1.6	2.851	1.908	3.251	1.808				3.251		**0.400**	**0.000**
1.75	1.75	0.6	2.4	3.251	1.808			3.251	0.000	1.750	3.692	0.000	**0.441**	**0.159**
2.00	2.00	0.6	2.4	3.692	1.722			3.692	0.000	2.000	4.114	0.000	**0.422**	**0.178**

Example 2. Horton. Assume the same rainfall hyetograph as for example 1 falls on a soil with Horton infiltration parameters, $f_o = 6$ cm/h, $f_1 = 1$ cm/h, $k = 2$ h^{-1}. Determine the runoff hyetograph using the Horton approach.

Solution. The solution is shown in table 5. Column 2 of table 5 shows the incremental rainfall and column 3 shows rainfall intensity. The solution follows the flowchart in Figure 42. After initializing (F=0) the infiltration capacity needs to be calculated (Box A) by solving equation (53, also given in table 3 column 1) implicitly. Define the function

$$g(f_c) = F - \frac{f_0 - f_c}{k} + \frac{f_1}{k} \ln\left(\frac{f_c - f_1}{f_0 - f_1}\right)$$

This can be solved for $g(f_c) = 0$ using the Solver function in Excel or a numerical solution method such as Newton Rhapson. $g(f_c)$ is shown in column 5. The result for F=0 is $f_c = 6$ shown in column 6. This is greater than the rainfall intensity (column 3) so ponding does not occur at time 0. We now move from box A in the flowchart (Figure 42) to box C:

$$F'_{t+\Delta t} = F_t + w_t \Delta t = 0 + 0.3 = 0.3 \, \text{cm} \quad \text{(column 7)}$$

This is the preliminary cumulative infiltration under the assumption of no ponding. The corresponding value of f'_c is obtained solving equation (53, given in table 3 column 1) implicitly again, this time showing $g(f'_c)$ in column 8 and the solution $f'_c = 5.5$ cm/h in column 9. This value is greater than w_t; therefore no ponding occurs during this interval and moving on to box E the cumulative infiltration is set to the preliminary value $F_{t+\Delta t} = F'_{t+\Delta t}$ as shown in column 15. Box F gives the infiltration (column 16) and runoff (column 17). The calculation then proceeds to box G where time is incremented and back to box A for the next time step. The same sequence is followed for the first four time steps where it is found that ponding does not occur up to 1.0 hours of rainfall.

During the fifth time interval (starting at 1.0 hours) when in box C we obtain $f'_c = 2.327$ cm/h as shown in column 9 of the table. This

value is less that w_t=2.8 cm/h for the interval 1 to 1.25 h so ponding starts during this interval. The calculation therefore proceeds to box D. The cumulative infiltration at ponding is given by equation (54, table 3 column 3)

$$F_p = \frac{f_0 - w}{k} - \frac{f_1}{k}\ln\left(\frac{w - f_1}{f_0 - f_1}\right) = \frac{6 - 2.8}{2} - \frac{1}{2}\ln\left(\frac{2.8 - 1}{6 - 1}\right) = 2.111\,\text{cm}$$

(column 10)

The partial time interval required for ponding is

$\Delta t' = (F_p\text{-}F_t)/w_t = (2.111 - 1.8)/2.8 = 0.111$ h. (column 11)

Ponding therefore starts at $1.0 + 0.111 = 1.111$ h as shown in column 12. Infiltration under ponded conditions occurs from 1.111 h to 1.25 h. The cumulative infiltration at the end of this interval is obtained by solving (56) for t_o implicitly then (57) for F (table 3, column 3). Define the function

$$h(t_0) = F_s - f_1(t_s - t_0) - \frac{(f_0 - f_1)}{k}(1 - e^{-k(t_s - t_0)})$$

and solve numerically for $h(t_0) = 0$. $h(t_0)$ is shown in column 14. This results in t_o=0.6 h (column 13) which in (57) gives

$F_{t+\Delta t}$=2.468 cm. (column 15)

The infiltration in this time interval is therefore (column 16)

$f_t = F_{t+\Delta t} - F_t = 2.468 - 1.8 = 0.668$ cm

The rainfall is 0.7 cm so the runoff generated is 0.7-0.668 = 0.032 cm (column 17).

At the start of the sixth time interval (time = 1.25 h) the cumulative infiltration is 2.468 cm. This leads to an infiltration capacity solved for implicitly in equation (53, column 1 table 3) of 2.363 cm/h shown in column 6. This is already less than the rainfall rate (3.2 cm/h) for the sixth time interval so the calculation proceeds through box B on the flowchart. The procedure is exactly the same as for box D, except that the starting values F_s and t_s are taken as the beginning of the time step values (columns 10 and 12). There is no need to solve for the time when ponding starts during the interval. Numerical

solution of $h(t_0) = 0$ results in the same t_0 as in the previous time step. t_0 only increases following infiltration under non ponded conditions. Equation (57, table 3 column 3) is used to obtain $F_{t+\Delta t}$ given in column 15.

During the seventh time interval (starting at time =1.5 h) the rainfall rate reduces to 1.6 cm/h. At the start of this interval the cumulative infiltration is 2.986 cm and solving (53) implicitly the infiltration capacity is 1.827 cm/h (column 5). This is more than the rainfall rate, so in this time interval ponding ceases and all rainfall at the beginning of this time step infiltrates. The calculation enters box C of the flowchart and the preliminary cumulative infiltration at the end of the time interval is calculated (column 7)

$$F'_{t+\Delta t} = F_t + w_t \Delta t = 2.986 + 0.4 = 3.386 \text{cm}$$

Using this value in equation (53) gives (column 9) $f'_c = 1.510$ cm/h. This is less than the rainfall rate so ponding occurs part of the way through this interval, as was the case during the fifth time interval. The calculation proceeds through boxes D, F and G as for the fifth time interval. The time offset t_0 solution to $h(t_0) = 0$ (column 14) increases (slightly) from what it was previously.

During the eighth time interval (starting at time =1.75 h) the rainfall rate increases to 2.4 cm/h. At the start of this interval the cumulative infiltration is 3.383 cm and using equation (53) the infiltration capacity (column 6) is $f_c = 1.512$ cm/h. This is less than the rainfall rate, so ponding occurs again in this time interval, starting at the beginning of the time interval and the calculation proceeds through box B similar to the sixth time interval above, with infiltration and runoff given in columns 16 and 17.

The last time interval (starting at time = 2.00 h) is similar, with ponding throughout the interval. Figure 44 illustrates the rainfall hyetograph, infiltration capacity and runoff generated from this example.
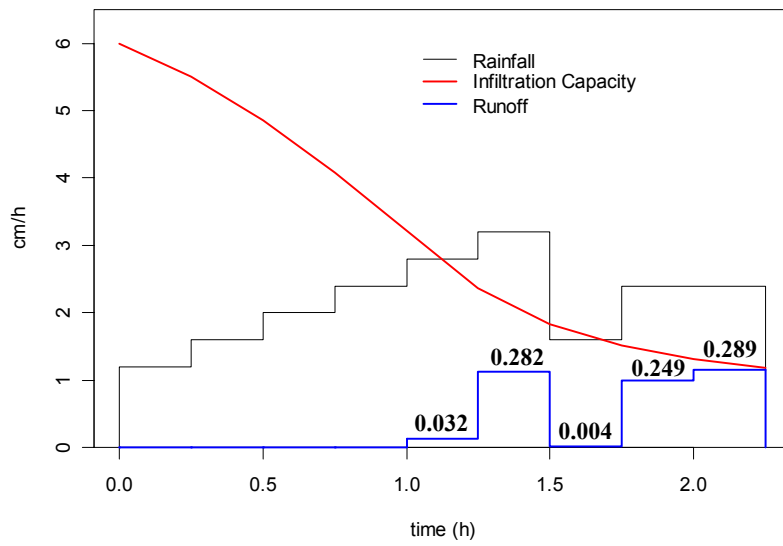
Figure 44. Rainfall Hyetograph, Infiltration Capacity and Runoff Generated in Example 2. Numbers are infiltration in cm in each interval.

Table 5. Calculation of runoff using the Horton infiltration equation.

Column 1	2	3	4	5	6	7	8	9	10	11	12	13	14	15	16	17
Time	Incremental Rainfall	Rainfall Intensity	F_t	$g(f_c)$	f_c	F'	$g(f_c')$	f_c'	F_p or F_s	dt'	t_s	t_o	$h(t_o)$	$F_{t+\Delta t}$	Infiltration	Runoff
(h)	(cm)	(cm/h)	(cm)		(cm/h)	(cm)		(cm/h)	(cm)	(h)	(h)	(h)		(cm)	(cm)	(cm)
0	0.3	1.2	0	0	6	0.300	8E-08	5.504						0.300	**0.300**	**0.000**
0.25	0.4	1.6	0.300	8E-08	5.504	0.700	4E-07	4.859						0.700	**0.400**	**0.000**
0.50	0.5	2	0.700	4E-07	4.859	1.200	2E-07	4.083						1.200	**0.500**	**0.000**
0.75	0.6	2.4	1.200	2E-07	4.083	1.800	2E-07	3.214						1.800	**0.600**	**0.000**
1.00	0.7	2.8	1.800	2E-07	3.214	2.500	3E-07	2.327	2.111	0.111	1.111	0.600	0.000	2.468	**0.668**	**0.032**
1.25	0.8	3.2	2.468	8E-07	2.363				2.468	0.000	1.250	0.600	0.000	2.986	**0.518**	**0.282**
1.50	0.4	1.6	2.986	3E-07	1.827	3.386	8E-07	1.510	3.260	0.171	1.671	0.611	0.000	3.383	**0.396**	**0.004**
1.75	0.6	2.4	3.383	6E-07	1.512				3.383	0.000	1.750	0.611	0.000	3.734	**0.351**	**0.249**
2.00	0.6	2.4	3.734	3E-07	1.311				3.734	0.000	2.000	0.611	0.000	4.045	**0.311**	**0.289**

Ponding Ponding (between 0.75 and 2.00)

Example 3. Philip. A rainfall hyetograph is given in column 2 of table 6. If this rain falls on a sandy loam, determine the runoff hyetograph using the Philip approach.

Solution. The solution is shown in table 6. From table 2, for a sandy loam, K_{sat} = 1.09 cm/h, θ_e = 0.412 and $|\psi_f|$ =11.01 cm. Assuming $\Delta\theta = \theta_e$ in equation (61) we get

$$S_p = (2K_{sat}\Delta\theta |\psi_f|)^{1/2}$$
$$= (2 \times 1.09 \times 0.412 \times 11.01)^{1/2} = 3.14 \, cm \, h^{-1/2}$$

Take K_p =K_{sat}/2 = 0.545 cm/h in the middle of the range from 1/3 K_p to 2/3 K_{sat} suggested by Sharma (1980). The solution follows the flowchart in Figure 42. Initially F=0, so f_c = ∞ (from 60) and ponding does not occur at time 0. The calculation moves from box A to box C in the flowchart.

$$F'_{t+\Delta t} = F_t + w_t \Delta t = 0 + 0.3 = 0.3 \, cm \qquad \text{(column 6)}$$

This is the preliminary cumulative infiltration under the assumption of no ponding. The corresponding value of f'_c is calculated using equation (60, table 3 column 1)

$$f_c(F) = K_p + \frac{K_p S_p}{\sqrt{S_p^2 + 4K_p F} - S_p}$$
$$= 0.545 + \frac{0.545 \times 3.14}{\sqrt{3.14^2 + 4 \times 0.545 \times 0.3} - 3.14} = 17.29 \, cm/h$$

as shown in column 7 of the table. This value is greater than w_t; therefore no ponding occurs during this interval and moving on to box E the cumulative infiltration is set to the preliminary value $F_{t+\Delta t} = F'_{t+\Delta t}$ as shown in column 12. Box F gives the infiltration (column 13) and runoff (column 14). The calculation then proceeds to box G where time is incremented and back to box A for the next time step. The same sequence is followed for the first four time steps where it is found that ponding does not occur up to 1.0 hours of rainfall.

During the fifth time interval (starting at 1.00 hours) when in box C
we obtain

$$f_c\,(F) = K_p + \frac{K_pS_p}{\sqrt{S_p^2 + 4K_pF} - S_p}$$

$$= 0.545 + \frac{0.545 \times 3.14}{\sqrt{3.14^2 + 4 \times 0.545 \times 2.5} - 3.14} = 2.765\,\text{cm/h}$$

as shown in column 7 of the table. This value is less that w_t=2.8
cm/h for the interval 1.0 to 1.25 h so ponding starts during this
interval. The calculation therefore proceeds to box D. The
cumulative infiltration at ponding F_p is given by (62, table 3, column
2)

$$F_p = \frac{S_p^2(w - K_p/2)}{2(w - K_p)^2} = \frac{3.14^2(2.8 - 0.545/2)}{2(2.8 - 0.545)^2} = 2.458\,\text{cm}$$

The partial time interval required for ponding is

$$\Delta t' = (F_p\text{-}F_t)/w_t = (2.458 - 1.8)/2.8 = 0.235\,\text{h}.$$

Ponding therefore starts at 1.0 + 0.235 = 1.235 h as shown in
column 10. Infiltration under ponded conditions occurs from 1.235
h to 1.25 h. The cumulative infiltration at the end of this interval is
obtained by solving (64, table 3 column 3) for t_o then (65, table 3
column 3) for F.

$$t_0 = t_s - \frac{1}{4K_p^2}\left(\sqrt{S_p^2 + 4K_pF_s} - S_p\right)^2$$

$$= 1.235 - \frac{1}{4 \times 0.545^2}\left(\sqrt{3.14^2 + 4 \times 0.545 \times 2.458} - 3.14\right)^2$$

$$= 0.749$$

$$F = S_p(t - t_0)^{1/2} + K_p(t - t_0)$$

$$= 3.14 \times (1.25 - 0.749)^{1/2} + 0.545 \times (1.25 - 0.749)$$

$$= 2.4997\,\text{cm}$$

This result is practically equivalent, but numerically slightly less than the cumulative rainfall of 2.5 cm up to this point. The infiltration in this time interval is therefore (column 13)

$$f_t = F_{t+\Delta t} - F_t = 2.4997 - 1.8 = 0.6997 \text{ cm}$$

The rainfall is 0.7 cm so the runoff generated is 0.7-0.6997 = 0.0003 cm (column 14), which is practically 0. The precision carried here is only for clarity in the calculations.

At the start of the sixth time interval (time = 1.25 h) the cumulative infiltration is 2.4997 cm. This leads to an infiltration capacity

$$
\begin{aligned}
f_c\,(F) &= K_p + \frac{K_p S_p}{\sqrt{S_p^2 + 4K_p F} - S_p} \\
&= 0.545 + \frac{0.545 \times 3.14}{\sqrt{3.14^2 + 4 \times 0.545 \times 2.4997} - 3.14} \\
&= 2.766 \text{ cm/h}
\end{aligned}
$$

This is already less than the rainfall rate (3.2 cm/h) for the sixth time interval so the calculation proceeds through box B on the flowchart. The procedure is exactly the same as for box D, except that the starting values F_s and t_s are taken as the beginning of the time step values (columns 8 and 10). There is no need to solve for the time when ponding starts during the interval.

During the seventh time interval (starting at time =1.5 h) the rainfall rate reduces to 1.6 cm/h. At the start of this interval the cumulative infiltration is 3.135 cm and using equation (60, table 3 column 1) the infiltration capacity is 2.359 cm/h (column 5). This is more than the rainfall rate, so in this time interval ponding ceases and all rainfall infiltrates (at least initially). The calculation enters box C of the

flowchart and the preliminary cumulative infiltration at the end of the time interval is calculated (column 6)

$$F'_{t+\Delta t} = F_t + w_t \Delta t = 3.135 + 0.4 = 3.535 \text{ cm}$$

Using this value in equation (60, table 3 column 1) gives (column 7) f_c'=2.177 cm/h. This is more than the rainfall rate so no ponding in this interval is confirmed, and the calculation proceeds through box E, F, G, resulting in no runoff being generated.

During the eighth time interval (starting at time =1.75 h) the rainfall rate increases to 2.4 cm/h. At the start of this interval the cumulative infiltration is 3.535 cm and using equation (60, table 3 column 1) (or recognizing the result from above) the infiltration capacity (column 5) is f_c=2.177 cm/h. This is less than the rainfall rate, so ponding occurs again, starting at the beginning of the time interval and the calculation proceeds through box B similar to the sixth time interval above, with infiltration and runoff given in columns 13 and 14.

The last time interval (starting at time = 2.00 h) is similar with ponding throughout the interval. Figure 45 illustrates the rainfall hyetograph, infiltration capacity and runoff generated from this example.
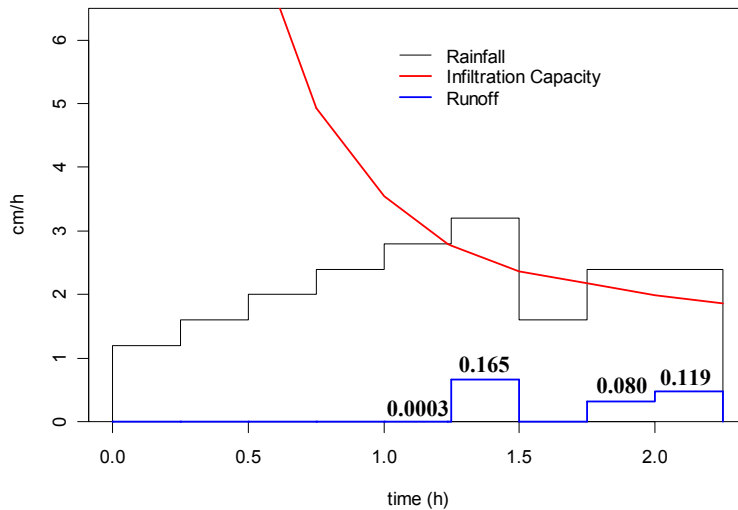
Figure 45. Rainfall Hyetograph, Infiltration Capacity and Runoff Generated in Example 3. Numbers are infiltration in cm in each interval.

Table 6. Calculation of runoff using the Philip infiltration equation.

Column 1	2	3	4	5	6	7	8	9	10	11	12	13	14
	Incremental Rainfall	Rainfall											
Time	Rainfall	Intensity	F_t	f_c	F'	f_c'	F_p or F_s	dt'	t_s	t_o	$F_{t+\Delta t}$	**Infiltration**	**Runoff**
(h)	(cm)	(cm/h)	(cm)	(cm/h)	(cm)	(cm/h)	(cm)	(h)	(h)	(h)	(cm)	**(cm)**	**(cm)**
0	0.3	1.2	0	∞	0.300	17.294					0.300	**0.300**	**0.000**
0.25	0.4	1.6	0.300	17.294	0.700	7.8711					0.700	**0.400**	**0.000**
0.50	0.5	2	0.700	7.8711	1.200	4.9218					1.200	**0.500**	**0.000**
0.75	0.6	2.4	1.200	4.9218	1.800	3.5417					1.800	**0.600**	**0.000**
1.00	0.7	2.8	1.800	3.5417	2.500	2.7655	2.458	0.235	1.235	0.749	2.4997	**0.6997**	**0.0003**
1.25	0.8	3.2	2.4997	2.7657			2.4997	0.000	1.250	0.749	3.135	**0.635**	**0.165**
1.50	0.4	1.6	3.135	2.359	3.535	2.1771					3.535	**0.400**	**0.000**
1.75	0.6	2.4	3.535	2.1771			3.535	0.000	1.750	0.822	4.055	**0.520**	**0.080**
2.00	0.6	2.4	4.055	1.9936			4.055	0.000	2.000	0.822	4.536	**0.481**	**0.119**

Ponding

Empirical and index methods

The Horton, Philip and Green-Ampt at a point infiltration models attempt to represent the physics of the infiltration process described by Richard's equation, albeit in a simplified way (although given the examples above it may not seem so simple). In many situations the data does not exist to support application of one of these approaches, or spatial variability over a watershed makes this impractical. Empirical and index methods are therefore still rather commonly used in practice, despite being lacking in theoretical basis.

The ϕ Index. The ϕ index method requires that a rainfall hyetograph and streamflow hydrograph are available. First baseflow needs to be separated from streamflow to produce the direct runoff hydrograph. Various methods for baseflow separation are illustrated in Figure 46. These are acknowledged as empirical and somewhat arbitrary. The ϕ index is that constant rate of abstractions (in/h or cm/h) that will yield an excess rainfall hyetograph (ERH) with a total depth equal to the depth of direct runoff over the watershed. The volume of loss is distributed uniformly across the storm pattern as shown in Figure 47. The ϕ index determined from a single storm is not generally applicable to other storms, and unless it is correlated with basin parameters other than runoff, it is of little value (Viessman et al., 1989).

(a) Straight line method.
(b) Fixed base method.
(c) Variable slope method.
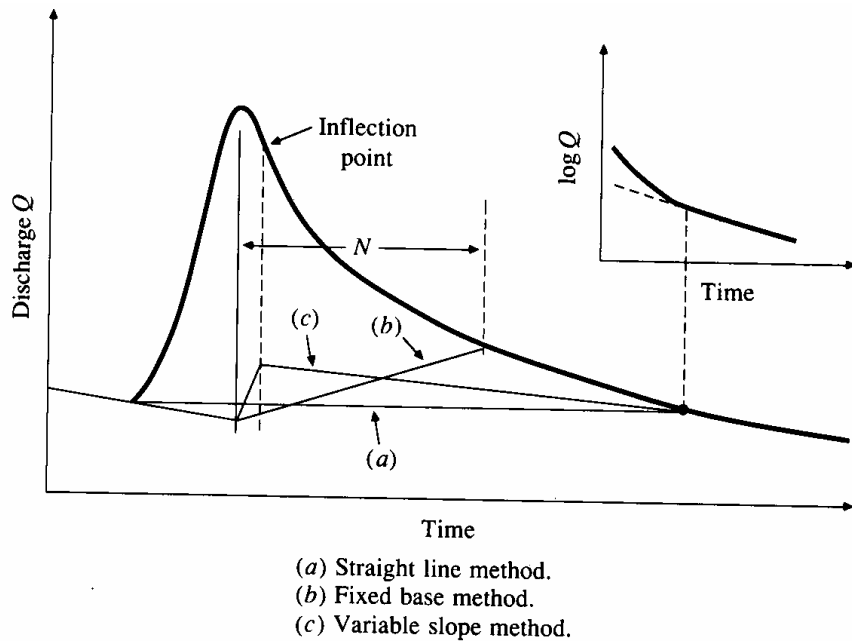
Figure 46. Baseflow Separation Techniques (from Chow et al, 1988).
Linsley et al. (1982) suggest as a rule of thumb N=0.2A, for A in square
miles and N in days for the fixed base method (b).
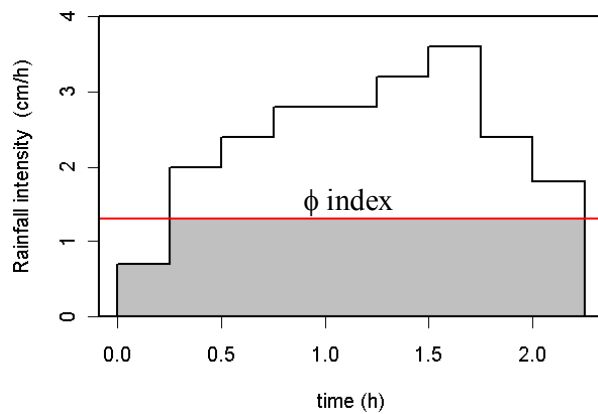
Figure 47. Representation of a ϕ index.

Runoff Coefficients. Abstractions may also be accounted for by
means of runoff coefficients. The most common definition of a
runoff coefficient is that it is the ratio of the peak rate of direct
runoff to the average intensity of rainfall in a storm. Because of

highly variable rainfall intensity, this value is difficult to determine from observed data. A runoff coefficient can also be defined to be the ratio of runoff to rainfall over a given time period. These coefficients are most commonly applied to storm rainfall and runoff, but can also be used for monthly or annual rainfall and streamflow data.

The SCS Method. The following description follows Chow et al. (1988). The Soil Conservation Service (1972) developed a method for computing abstractions from storm rainfall. For the storm as a whole, the depth of excess precipitation or direct runoff R is always less than or equal to the depth of precipitation P; likewise, after runoff begins, the additional depth of water retained in the watershed, F_a, is less than or equal to some potential maximum retention S. There is some amount of rainfall I_a (initial abstraction) for which no runoff will occur, so the potential runoff is P-I_a. The hypothesis of the SCS method is that the ratios of the two actual to the two potential quantities are equal, that is,

$$\frac{F_a}{S} = \frac{R}{P - I_a} \tag{66}$$

From the continuity principle

$$P = R + I_a + F_a \tag{67}$$

Combining (66) and (67) to solve for R gives

$$R = \frac{(P - I_a)^2}{P - I_a + S} \tag{68}$$

which is the basic equation for computing the depth of excess rainfall or direct runoff from a storm by the SCS method.

By study of results from many small experimental watersheds, an empirical relation was developed

$$I_a = 0.2\ S \tag{69}$$

On this basis

$$R = \frac{(P - 0.2S)^2}{P + 0.8S}$$ (70)

Plotting data for P and R from many watersheds, the SCS found curves of the type shown in Figure 48. To standardize these curves, a dimensionless curve number CN is defined such that $0 \leq CN \leq 100$. For impervious and water surfaces CN = 100; for natural surfaces CN < 100.
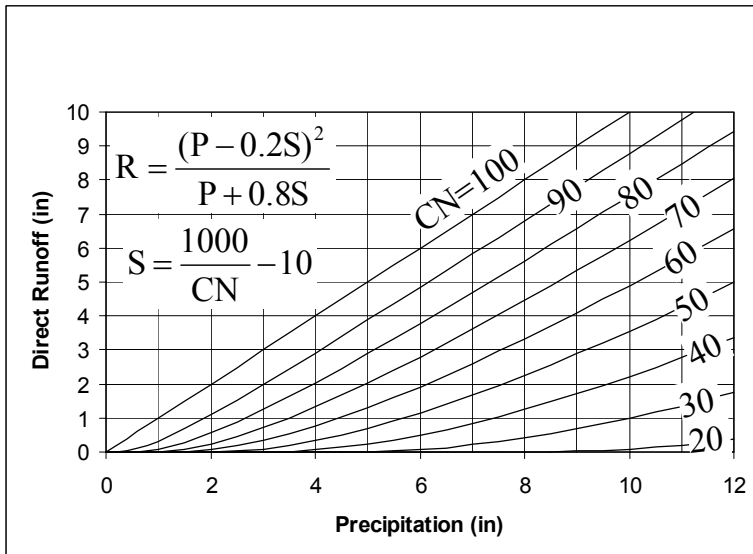
Figure 48. Solution to the SCS runoff equations.

The curve number and S are related by

$$S = \frac{1000}{CN} - 10$$ (71)

where S is in inches. The curve numbers shown in Figure 48 apply for *normal antecedent moisture conditions* (AMC II).

For dry conditions (AMC I) or wet conditions (AMC III), equivalent curve numbers can be computed by

$$CN(I) = \frac{4.2CN(II)}{10 - 0.058CN(II)} \tag{72}$$

and

$$CN(III) = \frac{23CN(II)}{10 + 0.13CN(II)} \tag{73}$$

The range of antecedent moisture conditions for each class is shown in table 7. Curve numbers have been tabulated by the Soil Conservation Service on the basis of soil type and land use. Four soil groups are used:

Group A: Low runoff potential. Soils having high infiltration capacity even if thoroughly wetted, such as deep sand, deep loess, aggregated silts.

Group B: Soils having moderate infiltration capacity if thoroughly wetted, such as shallow loess, aggregated silts.

Group C: Soils having low infiltration capacity if thoroughly wetted, such as clay loams, shallow sandy loam, soils low in organic content and soils usually high in clay.

Group D: High runoff potential. Soils having very low infiltration capacity if thoroughly wetted consisting chiefly of soils that swell significantly when wet, heavy plastic clays, and certain saline soils.

The values of CN for various land uses on these soil types are given in table 8. For a watershed made up of several soil types and land uses a composite average CN is customarily used, despite the nonlinearity of (71) and (70). The SCS curve number methods are empirical and limited in their physical basis, but are often used in practice due to the availability of CN values in soils maps and databases such as STATSGO (USDA-NRCS Soil Survey Division).

Table 7. Classification of antecedent moisture classes (AMC) for the SCS method of rainfall abstraction.

	Total 5-day antecedent rainfall (in)	
AMC group	Dormant Season	Growing Season
I	Less than 0.5	Less than 1.4
II	0.5 to 1.1	1.4 to 2.1
III	Over 1.1	Over 2.1

Table 8. Runoff curve numbers for selected agricultural, suburban and urban land uses.

Land Use Description	Hydrologic Soil Group			
	A	B	C	D
Cultivated land: without conservation treatment	72	81	88	99
with conservation treatment	62	71	787	81
Pasture or range land: poor condition[1]	68	79	86	89
good condition[1]	39	61	74	80
Meadow: good condition	30	58	71	78
Wood or forest land: thin stand, poor cover, no mulch	45	66	77	83
good cover[2]	25	55	70	77
Open Spaces, lawns, parks, golf courses, cemeteries, etc.				
good condition: grass cover on 75% or more of the area	39	61	74	80
fair condition: grass cover on 50% to 75% of the area	49	69	79	84
Commercial and business areas (85% impervious)	89	92	94	95
Industrial districts (72% impervious)	81	88	91	93
Residential				
Average lot size Average % impervious				
1/8 acre or less 65	77	85	90	92
1/4 acre 38	61	75	83	87
1/3 acre 30	57	72	81	87
1/2 acre 25	54	70	80	85
1 acre 20	51	68	79	84
Paved parking lots, roofs, driveways, etc.	98	98	98	98
Streets and roads:				
paved with curbs and storm sewers	98	98	98	98
gravel	76	85	89	91
dirt	72	82	87	89

1. Poor and good condition here refers to hydrologic condition. Poor is highly grazed or compacted with low infiltrability, good is less disturbed with higher infiltrability.
2. Good cover is protected from grazing ant litter and brush cover soil

Antecedent Precipitation Index.

Antecedent precipitation methods have been empirically devised to account for the fact that the quantity of runoff from a storm depends on the moisture conditions of the catchment at the beginning of the storm. The precipitation summed over a past period of time is used as a surrogate for soil moisture. The Antecedent Precipitation Index I is computed at the end of each day t from

$$I_t = k\,I_{t-1} + P_t \tag{73}$$

where P_t is the precipitation during day t and k is a recession factor (typically in the range 0.85 to 0.98) representing a logarithmic decrease in soil moisture with time during periods of no precipitation. Infiltration equations based on the antecedent precipitation index take the form

$$f_c = f_1 + (f_0 - f_1)e^{-bI} \tag{74}$$

In antecedent precipitation index methods k, f_0, f_1, and b are empirically or statistically derived coefficients that may vary with season and soil type. Linsley et al. (1982) give further details of this method which has limited physical basis, but given here because it may still be encountered in use in certain situations.

Exercises

1. Consider a silty clay loam soil with the following properties:

Porosity	0.477
Air entry tension ψ_a (cm)	35.6
Pore size distribution index b	7.75
Residual moisture content θ_r	0.15

   Hydrostatic conditions exist over a water table 1.5 m deep.

   a) Calculate the **suction** and **moisture content** at depths of **0.5 m** and **1.25 m**, using the Brooks and Corey soil moisture characteristic equations as well as the Clapp and Hornberger simplifications.
   b) Plot a graph of the **soil moisture content** as a function of depth.
   c) Calculate the **soil moisture deficit**, i.e. the amount of water that could infiltrate before the occurrence of saturation excess runoff. Use the Brooks and Corey soil moisture characteristic equations

2. Consider a silty clay loam soil with the following properties

Porosity	0.477
K_{sat} (cm/h)	0.612
Air entry tension ψ_a (cm)	35.6
Pore size distribution index b	7.75
Initial moisture content	0.3

   a) Calculate ψ_f (cm) according to the Green – Ampt model.
   b) Given precipitation at a rate of 2 cm/h calculate the cumulative infiltration at ponding, F_p (cm),and time to ponding, t_p (h).
   c) Assume that this rainfall of 2 cm/h persists for 3 hours. Calculate the runoff produced in cm.
   d) Calculate the infiltration capacity, f_c (cm/h), at the end of this 3 hour period.

3. Consider a soil with the following properties pertaining to Philip's Infiltration Equation

   Sorptivity, S_p in Philip's equation $(cm/h^{0.5})$ 2.5
   Conductivity, K_p in Philip's equation (cm/h) 0.4

   a) Given precipitation at a rate of 2 cm/h calculate the cumulative infiltration at ponding, F_p (cm), and time to ponding, t_p (h).
   b) Calculate the time compression time offset, t_o (h):
   c) Assume that this rainfall of 2 cm/h persists for 3 hours. Calculate the runoff produced in cm:
   d) Calculate the infiltration capacity, f_c (cm/h), at the end of this 3 hour period using the cumulative infiltrated depth F (equation 60).
   e) Calculate the infiltration capacity, f_c (cm/h), at the end of this 3 hour period using equation (59) with $t-t_o$ substituted for t.

4. Consider a soil with infiltration governed by the Horton equation with parameters

   $f_o = 4$ cm/h
   $f_1 = 1$ cm/h
   $k = 1.3$ h^{-1}

   a) Given precipitation at a rate of 2 cm/h calculate the cumulative infiltration at ponding, F_p (cm), and time to ponding t_p (h).
   b) Calculate the time compression time offset, t_o (h).
   c) Assume that this rainfall of 2 cm/h persists for 3 hours. Calculate the runoff produced in cm.
   d) Calculate the infiltration capacity, f_c (cm/h), at the end of this 3 hour period using the cumulative infiltrated depth F (implicit equation 53).
   e) Calculate the infiltration capacity, f_c (cm/h), at the end of this 3 hour period using equation (50) with $t-t_o$ substituted for t.

5. Consider a soil with properties

   Porosity   0.477
   K_{sat} (cm/h)   0.612
   $|\psi_a|$ (cm)   35.6
   b   7.75

   a) Use equation (44) to evaluate $|\psi_f|$ from the air entry pressure.
   b) Use the Clapp and Hornberger (1978) simplifications of Brooks and Corey functions (equation 27) to evaluate the

moisture content at field capacity defined as moisture content when $\psi = -340$ cm.

c) Assume field capacity initial conditions to evaluate the Green-Ampt parameter $P=|\psi_f|\Delta\theta$.

d) Use the Green-Ampt model (equation 42) to plot a graph of infiltration capacity as a function of infiltrated volume for this soil.

e) Given the following rainfall hyetograph calculate the ponding, infiltration and runoff generated in each time step.

Time (hours)	0-1	1-2	2-3	3-4
Rainfall intensity (cm/hr)	1	2	4	1.4

6. Consider a soil with properties

Porosity	0.477
K_{sat} (cm/h)	0.612
$|\psi_f|$ (cm)	145.2
Initial moisture content θ_o	0.3

a) Estimate $K_p = K_{sat}/2$ and S_p from equation (61).

b) Use the Philip model (equation 60) to plot a graph of infiltration capacity as a function of infiltrated volume for this soil.

c) Given the following rainfall hyetograph calculate the ponding, infiltration and runoff generated in each time step.

Time (hours)	0-1	1-2	2-3	3-4
Rainfall intensity (cm/hr)	1	2	4	1.4

7. Consider the following storm:

Time (hours)	0-0.5	0.5-1	1-1.5
Rainfall intensity (cm/hr)	5	3	1.5

Horton's equation is applicable with f_o = 6 cm/h, f_1 = 1.06 cm/h and k = 2.3 h^{-1} .

a) Plot a graph of infiltration capacity as a function of infiltrated volume for this soil.

b) Determine the infiltration and runoff generated in each half hour increment. Plot your results. State the total depths of runoff and infiltration. Indicate the times when there is ponding.

8. Consider the following rainfall-runoff data on a watershed with area 0.2 mi^2.

Time (h)	1	2	3	4	5	6	7
Rainfall rate (in/h)	1.05	1.28	0.8	0.75	0.7	0.6	0
Direct runoff (cfs)	0	30	60	45	30	15	0

a) Calculate the volume of direct runoff from this watershed in ft^3. Do this by summing the cfs flows and multiplying by the number of seconds in an hour (3600).

b) Calculate the per unit area depth of direct runoff by dividing your answer in (a) by the basin area. Express your answer in inches. (There are 5280 ft to a mile and 12 in to a foot).

c) Calculate the total storm infiltration loss by subtracting the direct runoff (from b) from the total number of inches of precipitation.

d) Referring to figure 47 apportion this loss over the time steps where there is precipitation to estimate a ϕ-index from this storm. [Hint. In some time steps the rainfall rate will be less than the ϕ-index. You need to accommodate this in your calculations recognizing that in these cases the infiltration is the lesser of rainfall rate and ϕ-index.]

e) Determine the rainfall excess generated in each time step.

9. Compute the runoff from a 7 in rainfall on a watershed that has hydrologic soil groups that are 40% group A, 40% group B, and 20% group C interspersed throughout the watershed. The land use is 90% residential area that is 30% impervious and 10% paved roads with curbs. Assume AMC II conditions.

a) Report the average curve number.

b) Report the runoff in inches.

References

Bras, R. L., (1990), Hydrology, an Introduction to Hydrologic Science, Addison-Wesley, Reading, MA, 643 p.

Celia, M. A., E. T. Bouloutas and R. L. Zarba, (1990), "A General Mass-Conservative Numerical Solution for the Unsaturated Flow Equation," Water Resour. Res., 26(7): 1483-1496.

Chow, V. T., D. R. Maidment and L. W. Mays, (1988), Applied Hydrology, McGraw Hill, 572 p.

Dingman, S. L., (2002), Physical Hydrology, 2nd Edition, Prentice Hall, 646 p.

Dunne, T. and L. B. Leopold, (1978), Water in Environmental Planning, W H Freeman and Co, San Francisco, 818 p.

Eagleson, P. S., (1970), Dynamic Hydrology, McGraw-Hill Book Company, 462 p.

Gardner, W. and J. A. Widstoe, (1921), "Movement of Soil Moisture," Soil Sci., 11: 215-232.

Gerald, C. F., (1978), Applied Numerical Analysis, 2nd Edition, Addison Wesley, Reading, Massachusetts, 518 p.

Green, W. H. and G. Ampt, (1911), "Studies of Soil Physics. Part I - the Flow of Air and Water through Soils," J. Agric. Sci, 4: 1-24.

Horton, R. E., (1939), "Approach toward a Physical Interpretation of Infiltration Capacity," Proc. Soil Sci. Soc. Am., 23(3): 399-417.

Linsley, R. K., M. A. Kohler and J. L. H. Paulhus, (1982), Hydrology for Engineers, 3rd Edition, McGraw-Hill, New York, 508 p.

Mein, R. G. and C. L. Larson, (1973), "Modeling Infiltration During a Steady Rain," Water Resources Research, 9: 384-394.

Parlange, J.-Y., W. L. Hogarth, D. A. Barry, M. B. Parlange, R. Haverkamp, P. J. Ross, T. S. Steenhuis, D. A. DiCarlo and G. Katul, (1999), "Analytical Approximation to the Solutions of Richards' Equation with Applications to Infiltration, Ponding, and Time

Compression Approximation," <u>Advances in Water Resources</u>, 23: 189-194.

Philip, J. R., (1957), "The Theory of Infiltration: 1. The Infiltration Equation and Its Solution," <u>Soil Sci.</u>, 83(5): 345-357.

Philip, J. R., (1969), "Theory of Infiltration," in <u>Advances in Hydroscience</u>, Edited by V. t. Chow, Vol 5, Academic Press, New York, p.215-297.

Rawls, W. J., L. R. Ahuja, D. L. Brakensiek and A. Shirmohammadi, (1993), "Infiltration and Soil Water Movement," in <u>Handbook of Hydrology, Chapter 5</u>, Edited by D. R. Maidment, McGraw-Hill, New York.

Rawls, W. J., D. L. Brakensiek and N. Miller, (1983), "Green-Ampt Infiltration Parameters from Soils Data," <u>J Hydraul. Div. Am. Soc. Civ. Eng.</u>, 109(1): 62-70.

Sharma, M. L., G. A. Gander and G. C. Hunt, (1980), "Spatial Variability of Infiltration in a Watershed," <u>Journal of Hydrology</u>, 45: 101-122.

Smith, R. E., K. R. J. Smettem, P. Broadbridge and D. A. Woolhiser, (2002), <u>Infiltration Theory for Hydrologic Applications</u>, Water Resources Monograph 15, American Geophysical Union, Washington, DC, 212 p.

Soil Conservation Service, (1972), "Hydrology," Section 4 in <u>National Engineering Handbook</u>, U.S. Dept of Agriculture, Washington, DC.

USDA-NRCS Soil Survey Division, <u>National Statsgo Database</u>, <u>http://www.ftw.nrcs.usda.gov/stat_data.html</u>.

Viessman, W., G. L. Lewis and J. W. Knapp, (1989), <u>Introduction to Hydrology</u>, 3rd Edition, Harper & Row.

Youngs, E. G., (1964), "An Infiltration Method Measuring the Hydraulic Conductivity of Unsaturated Porous Materials," <u>Soil Science</u>, 97: 307-311.